Luminance and color inputs to mid-level and high-level vision

Ben J. Jennings

School of Psychology, University of Aberdeen, Aberdeen, UK
McGill Vision Research, Department of Ophthalmology, McGill University, Montreal, QC, Canada

Jasna Martinovic

School of Psychology, University of Aberdeen, Aberdeen, UK

We investigated the interdependence of activity within the luminance (L + M) and opponent chromatic (L − M and S − [L + M]) postreceptoral mechanisms in mid-level and high-level vision. Mid-level processes extract contours and perform figure-background organization whereas high-level processes depend on additional semantic input, such as object knowledge. We collected mid-level (good/poor continuation) and high-level (object/nonobject) two-alternative forced-choice discrimination threshold data over a range of conditions that isolate mechanisms or simultaneously stimulate them. The L − M mechanism drove discrimination in the presence of very low luminance inputs. Contrast-dependent interactions between the luminance and L − M as well as combined L − M and S − (L + M) inputs were also found, but S − (L + M) signals, on their own, did not interact with luminance. Mean mid-level and high-level thresholds were related, with luminance providing inputs capable of sustaining performance over a broader, linearly corresponding range of contrasts when compared to L − M signals. The observed interactions are likely to be driven by L − M signals and relatively low luminance signals (approximately 0.05–0.09 L + M contrast) facilitating each other. The results are consistent with previous findings on low-level interactions between chromatic and luminance signals and demonstrate that functional interdependence between the geniculate mechanisms extends to the highest stages of the visual hierarchy.

Introduction

Detection and identification of objects are crucial functions of visual perception. To achieve these goals, multiple parallel pathways process incoming visual information. Although visual processing is not truly serial, it is often conceptualized as several rapidly occurring, hierarchically organized steps: low-level, mid-level, and high-level processes. Low-level vision analyzes elementary features, such as local color, luminance, motion, or binocular disparity, and mid-level vision extracts edges and segments surfaces, which are layered via figure-background organization processes, such as edge-region grouping (Palmer & Brooks, 2008). Finally, high-level processing depends on the input from stored representations leading to object classification.

Structurally, three different pathways are distinguished at the level of the lateral geniculate nucleus. The magnocellular pathway processes luminance information only, and the parvocelluar and koniocellular pathways also subserve color processing (Kulikowski, 2003). These pathways roughly correspond to the three independent geniculate mechanisms identified electrophysiologically in the macaque (Derrington, Krauskopf, & Lennie, 1984). Cone-opponent L − M signals are processed by the parvocellular layers, and S − (L + M) signals are processed by middle koniocellular layers (Tailby, Szmajda, Buzas, Lee, & Martin, 2008). Luminance signals (L + M) can be processed by both magnocellular and parvocellular layers as the parvocellular neurons are able to multiplex L − M and luminance information (Kingdom & Mullen, 1995). Cortically, S − (L + M), L − M, and L + M signals start interacting at the level of V1 so that most of the early visual cortex contains neurons that are tuned to both color and luminance (for a review, see Solomon & Lennie, 2007).

A major goal of vision research is to investigate the independence and interaction of activity within different parallel visual pathways and to follow the transformation of visual information at various stages of visual processing. Interactions between luminance and color processing have been studied in low-level and mid-level vision. Low-level chromatic and achromatic

Citation: Jennings, B. J., & Martinovic, J. (2014). Luminance and color inputs to mid-level and high-level vision. *Journal of Vision*, *14*(2):9, 1–17, http://www.journalofvision.org/content/14/2/9, doi:10.1167/14.2.9.

doi: 10.1167/14.2.9 Received February 24, 2013; published February 11, 2014 ISSN 1534-7362

processing has been investigated extensively in human observers and other mammals (e.g., Crognale, 2002; McKeefry, Murray, & Kulikowski, 2001; Vidyasagar, Kulikowski, Lipnicki, & Dreher, 2002). Initially, psychophysical investigations compared performance of the luminance channel with that of the chromatic channels in order to assess if they are equally able to sustain spatial and temporal vision (for a review, see Gegenfurtner & Kiper, 2003). As discussed by Shevell and Kingdom (2008), recently, the focus has shifted to interactions between chromatic and luminance channels in form perception in order to gain more insights into processes that concurrently analyze luminance and chromatic properties of complex scenes. Psychophysical studies demonstrated that, although the coding of elementary visuospatial features defined by chromatic and achromatic signals seems to be independent at the detection threshold, it is subject to highly nonlinear interactions (inhibitory or facilitatory) at suprathreshold levels (for a review, see Kulikowski, 2003). Studies on simultaneous overlay contrast masking found asymmetric interactions between color and luminance in low-level vision: Suprathreshold luminance pedestals generally facilitated L − M chromatic detection while suprathreshold chromatic signals masked luminance-defined stimuli at higher spatial frequencies (Cole, Stromeyer, & Kronauer, 1990; Switkes, Bradley, & DeValois, 1988). An EEG study with suprathreshold contrasts also found facilitatory effects between chromatic and luminance information with S-cone inputs able to modify the luminance signal (Victor, Purpura, & Conte, 1998). In addition, studies on contour integration demonstrated that the processing of contours in mid-level vision could be subserved by both achromatic and chromatic mechanisms at very similar levels of performance due to the reliance of the mechanism on a common contour-integration process (Mathes & Fahle, 2007; Mullen, Beaudot, & McIlhagga, 2000). Chromatic signals also sustained the processing of Glass pattern stimuli similarly to luminance signals (Mandelli & Kiper, 2005; Wilson & Switkes, 2005), meaning that both path and texture processing could be driven by chromatic inputs. Pearson and Kingdom (2002) had previously demonstrated that chromatic and luminance signals are pooled by a common mechanism in texture processing.

To our knowledge, studies that relate the role of different psychophysical channels and visual pathways in mid-level and high-level vision have not yet been performed. Although achromatic and chromatic information are both crucial for everyday vision, their contributions differ with luminance considered to be more relevant for rapid processing of edges, contours, shape, and motion and color more relevant for segmentation of visual scenes into surfaces (Palmer, 1999). Object classification is an accurate and rapid process with studies showing that representation is generally accomplished within the initial 200–300 ms of processing time (for a review, see DiCarlo, Zoccolan, & Rust, 2012). Such speed of object classification is thought to be largely driven by luminance information. According to one influential model, the magnocellular pathway rapidly projects initial shape information obtained from luminance detectors into the prefrontal cortex, which subsequently constrains processing in posterior representational areas (Bar, 2003; Bar et al., 2006; Kveraga, Boshyan, & Bar, 2007). This is in line with the findings of Martinovic, Mordal, and Wuerger (2011) that object-selective modulations of the N1 component of the event-related potential (ERP) occurred only for full-information stimuli (both achromatic and chromatic) but not for purely chromatic stimuli. Furthermore, although luminance signals are not necessary for figure-background organization, their presence allows object representations to enact an early influence on figure-background organization (Peterson & Gibson, 1993, 1994). It is therefore very important to establish the contributions of both chromatic and achromatic signals to high-level vision and relate them to mid-level processes.

Hansen and Gegenfurtner (2009) looked at the role of chromatic information in the analysis of natural scene images by assessing the amount of shared information between different mechanisms. They found that luminance and chromatic edge processing are largely independent and argued that these mechanisms have evolved in order to provide complimentary linearly additive cues in scene segmentation. However, this study relied on image statistics; additional information brought about by color could be magnified in cortical processing. For example, the chromatic L − M mechanism possesses not only surface-color detectors, but also edge detectors that project to the upper layers of V1 (for a review, see Shapley & Hawken, 2011). L − M edge detectors were largely found to be orientation selective, and surface-color detectors were not orientation selective. In line with the special role of chromatic edges, studies on human participants that included both information on object contours and information on surfaces of objects have shown that processing of color or texture as surface cues were largely independent from form processing (Cant, Large, McCall, & Goodale, 2008); this could possibly be due to the additional importance of the chromatic content of a scene during the process of segmentation. However, the role of chromatic signals in shape processing should not be neglected as discrimination of global shapes can be sustained by all three channels with luminance being most effective, L − M information being less effective, and S − (L + M) being least effective (Mullen & Beaudot, 2002). In their study, Mullen and Beaudot (2002) only looked at performance driven by stimuli

that isolated the three mechanisms. The level of integration between chromatic and achromatic information in object processing is therefore not yet fully known. To our knowledge, this study is the first attempt to assess if information carried by different parallel pathways is subjected to interactions using mid-level and high-level visual processing tasks. The main objective is to investigate the interactions between psychophysical channels that are associated with different parallel visual pathways at the high-level stage of the visual-processing hierarchy and relate them to the mid-level process of good continuation, which is considered as one of the three most important mid-level processes for object classification (for a review, see Goldstone, Gerganov, Landy, & Roberts, 2009). S-cone contributions to high-level vision, in particular, have not yet been studied extensively, but Martinovic et al. (2011) found them to be less effective for sustaining accurate and fast object classification even at supra-threshold levels.

Using psychophysical measurements, we assessed the efficiency of each of the geniculate mechanisms separately and in combination, focusing on the interactions between luminance and chromatic information in a high-level object/nonobject discrimination task and a mid-level good continuation discrimination task. We defined an interaction between chromatic and luminance channels as a significant difference in threshold contrast in each of the stimulated channels when compared to channel-isolating threshold contrast. If less contrast is needed when multiple channels are stimulated that would imply facilitation; more contrast being needed would imply suppression. Although the mid-level task assessed thresholds for establishing the presence of good continuation, the high-level task involved stimuli that already possessed good continuation, requiring additional processes, such as assessment of further objecthood properties and/or actual object categorization. By comparing the mid-level and high-level thresholds, we will be able to relate the high-level stage of processing to continuation processes. Good continuation contributes to contour integration, a mid-level figure-background process that has already been examined in previous work on chromatic channels (e.g., Beaudot & Mullen, 2001, 2003; Mullen et al., 2000). In order for mid-level and high-level stimuli to be comparable, they both consisted of Gaborized outlines. It was expected that the contrasts required for discrimination threshold would be lower for the mid-level task, reflecting the additional difficulty involved in the high-level object discrimination task. It was also expected that interactions would be observed between L − M and luminance mechanisms due to the presence of L − M edge detectors along with some evidence of S-cone luminance boosting (Victor et al., 1998).

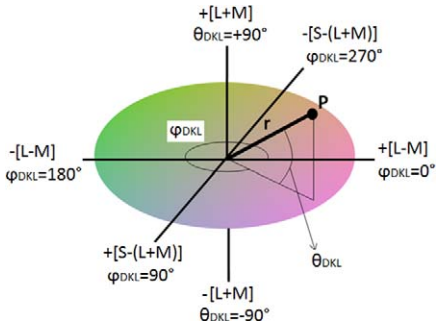

Figure 1. The DKL color space with its three perpendicular axes corresponding to the L − M, S − (L + M), and L + M mechanisms was used to specify the chromatic and luminance conditions (see Table 1). Point P is described by DKL (r, ϕ_{DKL}, θ_{DKL}), where r is its Euclidean distance in three-dimensional space from the center located at (0, 0, 0), ϕ_{DKL} is its angle of azimuth, and θ_{DKL} is its angle of elevation. The angle of azimuth defines the chromaticity. The angle of elevation defines the relative amount of luminance at point P with larger angles corresponding to more luminance contrast.

Methods

Participants

Forty-seven participants took part in the study in total. Twenty took part in the main experiment, but five of them were excluded from data analysis (see Heterochromatic flicker photometry, Procedure, and Data analysis sections for more details on exclusion criteria). Twelve took part in a subsequent control experiment with a different order of color-luminance conditions. Finally, 15 took part in the follow-up experiment with increased luminance angle resolution, but five of them had to be excluded due to some missing data (see Procedure section for more details). Participants in the main experiment were reimbursed for their time and effort, and participants in the control and follow-up experiments received class credit. Each participant reported normal or corrected-to-normal visual acuity and had normal color vision as assessed with the Cambridge Colour Test (Regan, Reffin, & Mollon, 1994). The study was approved by the ethics committee of the School of Psychology, University of Aberdeen.

DKL color space

The DKL color space (Derrington et al., 1984) was used to describe the chromatic properties of the stimuli. Figure 1 shows a representation of the DKL color space, indicating the two chromatic (L − M and S − [L

Condition	DKL chromatic angle (°)	DKL luminance angle (°)	Mechanism stimulated
1	90/270	0	S – (L + M)
2	0/180	0	L – M
3	0	±90	L + M
4	90/270	±30	S – (L + M) & L + M
5	90/270	±60	S – (L + M) & L + M
6	0/180	±30	L – M & L + M
7	0/180	±60	L – M & L + M
8	135/315	0	L – M & S – (L + M)
9	135/315	±30	L – M & S – (L + M) & L + M
10	135/315	±60	L – M & S – (L + M) & L + M

Table 1. Summary of the 10 chromatic and luminance conditions, defined in terms of the DKL color space.

+ M]) mechanisms and the luminance mechanism (L + M), along with a vector (P) defining a particular chromaticity and luminance with a radius r, chromatic angle ϕ_{DKL}, and luminance elevation θ_{DKL}. The chromatic and luminance components of the stimuli were defined so as to excite the L − M (reddish-greenish), S − (L + M) (yellowish-bluish), or L + M (luminance) mechanisms, either in isolation or combined at different levels of DKL elevation. Such choice of stimulus parameters allowed us to test stimuli with different ratios of chromatic and luminance content with higher DKL elevation leading to more luminance being present in a stimulus of the same radius. The DKL space was implemented in the Colour Toolbox (CRS, UK; Westland, Ripamonti, & Cheung, 2012) using measurements of the spectra of the monitor phosphors taken by a SpectroCAL (CRS, UK) and cone fundamentals (Stockman & Sharpe, 2000; Stockman, Sharpe, & Fach, 1999).

Stimuli were presented in 10 different chromatic and luminance conditions: The L − M, S − (L + M), and L + M channels were tested in isolation; the two chromatic channels were combined and tested at isoluminance; L − M and S − (L + M) were combined with an L + M luminance signal with DKL luminance elevations of $\theta_{DKL} = 30°$ and 60°; and finally, all three channels were combined at $\theta_{DKL} = 30°$ and 60°. Table 1 summarizes the 10 conditions in terms of their DKL parameters. A uniform background located at DKL(r, ϕ_{DKL}, θ_{DKL}) = (0, 0, 0) was used throughout the experiments; this corresponded to CIE 1931 xy of 0.290, 0.321 with a luminance of 51.6 cd m^{-2}.

Stimuli

Two stimulus sets were produced corresponding to mid-level and high-level visual processes. The mid-level stimuli were a set of contours with and without good continuation, and the so-called high-level stimuli were a set of nameable objects and unnameable "nonobjects." All stimuli were composed of a series of Gabor patches (see Figure 2), as defined by Equation 1.

$$g(x, y, \theta) = c \sin(2\pi f(x \sin\theta + y \cos\theta) + \varphi)\exp - \left(\frac{x^2 + y^2}{2\sigma^2}\right) \quad (1)$$

In Equation 1, x,y are coordinates that are used to define locations within the Gabor patch relative to its center. The Gabor patch orientation is given by θ. The Gabor phase offset (φ) was fixed at 0.25 (≡90°) corresponding to a center-symmetric profile. The spatial frequency ($f = 3.0$) was chosen so that roughly equal contrast dependence of orientation sensitivity across the cone classes would be maintained. Wuerger and Morgan (1999) found that for L − M and L + M signals this occurs at ~2 cpd, but a slightly higher frequency of 3 cpd was used in order to take into account the ecological consideration that luminance contrast sensitivity is highest between 3 and 5 cpd in the general population (Campbell & Robson, 1968), thus making these signals more relevant for everyday human vision. The Gabor patches' Gaussian envelope had a standard deviation of $\sigma = 0.067°$, ~20% of the Gabor size that subtended ~0.35° of visual angle with a spatial aspect ratio of 1. Figure 2(f through i) shows some examples of the Gabor patches defined by contrasts along different DKL mechanisms (also see DKL color space section).

The mid-level stimuli were designed so as to tap into the Gestalt principle of good continuation. The stimuli were composed of series of Gabor patches that formed two contours, crossing each other at or near to the central fixation point. Figure 2a and b shows an example of the contours with and without good continuation. The two types of contour shared the same global spatial properties; they were both composed of Gabor patches that were orientated relative to their neighbors within the range of ±30°, and their center-to-center separation was ~1°. The contours with

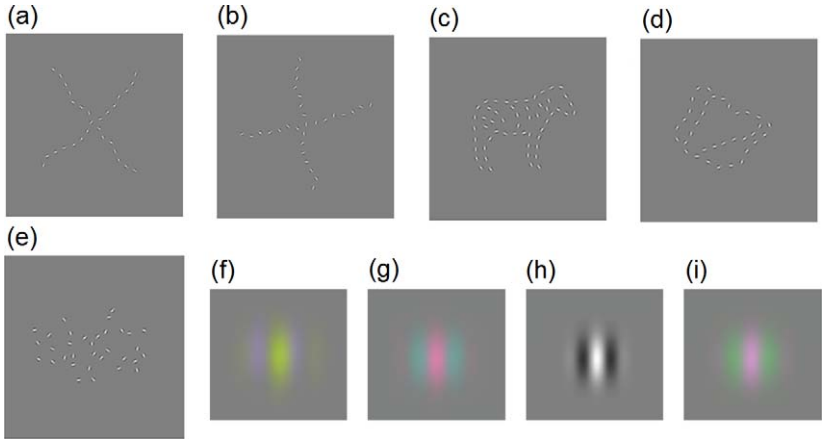

Figure 2. Examples of stimuli. (a) Two contours with good continuation, (b) two contours without good continuation, (c) a nameable object (a zebra), (d) a nonobject, and (e) a random patch of Gabors. The previous examples are all depicted using an achromatic Gabor patch. The following panels approximate the appearance of Gabor patches in some of the different experimental conditions: (f) S − (L + M) isolating condition, (g) L − M isolating condition, (h) L + M isolating condition, (i) combination of L − M and S − (L + M) at isoluminance.

good continuation had their Gabors orientated along the length of the contours (Figure 1a); the contours without continuation had their Gabors randomly orientated (Figure 1b). The contours were generated so that there was an equal chance of the global spatial distribution being orientated at any angle.

For the high-level stimuli, a large set of objects and nonobjects were produced; these were similar to the image library provided by Sassi, Vancleef, Machilsen, Panis, and Wagemans (2010). The object/nonobject stimuli were created by selecting suitable line images of familiar, nameable objects from various stimulus sets (Alario & Ferrand, 1999; Bates et al., 2003; Hamm & McMullen, 1998) and also by the manual digital drawing of additional line images. The lines of these images were replaced with a series of Gabor patches with the position of each Gabor patch predefined by hand in order to ensure that shape-defining lines were distributed along the relevant parts of the images. The corresponding nonobject images were created by distorting the line images of the objects until they became unrecognizable; this was achieved using image processing software (for more detail, see Martinovic et al., 2011). Figure 2c and d shows an example of an object (a zebra) and a nonobject, respectively. The process of scrambling the object images into nonobject images attempted to preserve some important attributes of the initial object images, including the visual complexity of the images as reflected in jpeg file size (Szekely & Bates, 2000) and their aspect ratio. It was ensured that some of the lines defined by Gabor patches were located near the fixation point (no further than approximately 1° away) in order to preclude the need for eye movements to object edges in low-contrast conditions close to threshold. The nonobjects were also constrained to have a closed outer contour in order to be consistent with that property of objecthood and preventing them from appearing as random clusters of Gabor patches with no global structure.

A pilot naming experiment was conducted with five participants, using the object/nonobject stimuli along with a third stimulus group composed of random clusters of Gabor patches, which acted as a control (Figure 2e). The task was to respond to each stimulus in turn by pressing a response box button that corresponded to either "Object," "Nonobject," or "Random." If the participants responded "Object" to a stimulus, they were then prompted to name it out loud, and the name was recorded by the experimenter. This allowed us to single out object stimuli that were classed as nonobjects (approximately 40 items), which were redrawn and retested. Only those object stimuli that were correctly identified with at least a 75% accuracy rate over the five participants were used, giving a set of 377 objects and 377 corresponding nonobjects. The final piloted set of object stimuli subtended a width and height of 6.7° ± 1.1° and 2.9° ± 1.0° (mean ± *SD*), respectively. The nonobject stimuli subtended a width and height of 7.6° ± 0.9° and 2.8° ± 0.8° (mean ± *SD*), respectively. Subsequently, a fast Fourier transform analysis of the stimuli was performed in Matlab (Mathworks, Natick, MA) to assess if there were differences between the two stimulus groups in dominant line orientation (vertical/horizontal or oblique). A permutation test ($n = 5{,}000$) demonstrated that the object stimuli contained significantly ($p < 0.05$) more vertical and horizontal components. Vertical and horizontal components were also pronounced in line drawings of objects previously used by Martinovic et al. (2011).

Apparatus

The experiment was conducted using a Dell PC with a visual stimulus generator (VISaGe; CRS, UK). The stimuli were displayed on a 21-in. Viewsonic P227f CRT Monitor calibrated with a ColorCAL 2 (CRS, UK) and controlled by the VISaGe system. CRS Toolbox and CRS Colour Toolbox for Matlab (Mathworks, Natick, MA) were used to run the experiment. Participants were seated in a dark room 80 cm in front of the monitor, which was the only source of light. They gave their responses using a Cedrus RB-530 button box (San Pedro, CA).

Heterochromatic flicker photometry (HCFP)

Individual differences in the luminous efficiency function (Wyszecki & Stiles, 2000) can result in a small luminance signal being present within the nominally isoluminant chromatic signals. In order to adjust for participants' individual points of isoluminance, HCFP (Walsh, 1958) was used. HCFP utilizes the difference in temporal resolution of the luminance channel compared to the chromatic channels, the luminance channel being capable of higher temporal resolution and hence able to process higher frequency flicker. Therefore, if a participant can adjust the relative amounts of luminance within a 20-Hz chromatically flickering set of Gabor patches so that the perception of flicker is minimized, the luminance difference will also be minimized, providing an isoluminant correction for individuals. Although some questions can be raised about the suitability of HCFP for setting isoluminance points for static stimuli, L- and M-cone inputs into the luminance mechanism change as a function of temporal frequency most prominently between 4 and 12 Hz, but at 20 Hz these differences become small (Stromeyer, Chaparro, Tolias, & Kronauer, 1997; see also Gegenfurtner & Hawken, 1995). Furthermore, HCFP yields very similar results to the minimally distinct border technique (Kaiser, 1971; Kaiser et al., 1990; Wagner & Boynton, 1972).

In the DKL space, HCFP correction can be applied by adjusting the angle of elevation of the isoluminant plane. The three isoluminant conditions used in the experiment were L − M and S − (L + M) in isolation as well as a combination of both L − M and S − (L + M). All participants reported that, by adjusting the luminance levels, they could find a setting at which the flickering stimulus became minimally visible or even completely nulled for each of the three conditions. Each participant repeated this task eight times for each condition. A basic outlier rejection method was performed: The lowest and highest values were eliminated from the set, and the mean of the remaining six determined, these were then applied as corrections for each individual participant during threshold measurements within the DKL isoluminant plane.

According to the study design, combined luminance and chromatic stimuli were to be presented at elevations of 30° and 60° with the part of the Gabor patch with the azimuth of 0° (L − M increment), 315° (combined L − M increment and S − [L + M] decrement), and 270° (S − [L + M] decrement) being made more luminant and the polar opposite being made less luminant. The choices of the part of the Gabor patch that was to be made more luminant were made based on evidence of cone inputs into the luminance mechanism (Brainard et al., 2000; Dobkins, Thiele, & Albright, 2000). Because the majority of participants would require the L − M increment to be reduced in luminance in order to achieve isoluminance, our choice of it as the brighter of the two would, at worst, lead to an underestimation of any color and luminance interactions observed in the study using different DKL elevations. However, for participants with a DKL elevation close to 30°, the combined L − M and luminance condition at 30° would be effectively isoluminant. In order to prevent this confound from influencing the results, only those participants with a correction of less that $\theta_{DKL} = 15°$ in the L − M direction were selected to take part. This was to ensure a sufficiently large separation between the corrected isoluminant conditions and the conditions that combined a chromatic signal along with a luminance signal. The luminance angles of the participants for the L − M condition are shown in Supplementary Figure 1. As can be seen from this figure, three participants were rejected at this stage.

Procedure

Threshold measurements using a two-interval forced-choice procedure were performed. The participant's task was to identify which interval contained either the contour with good continuation (mid-level) or the object (high-level). Two staircases, controlled through the Palamedes Toolbox (Kingdom & Prins, 2009) were run in parallel, each staircase modulating the individual Gabor patches with opposite contrast polarities, e.g., +(L − M) and −(L − M).

Each staircase consisted of 25 trials. Within each trial, the first stimulus was presented for 1200 ms, followed by 1000 ms of fixation, followed by the second stimulus for 1200 ms. After the second stimulus was displayed, the fixation cross remained on screen until a response was given by the participant before starting the next trial. The participants were instructed to guess if they were unable to determine which interval contained the contour with good continuation or the object. No feedback on accuracy was given during the experiment in order to lessen explicit learning of object/nonobject category characteristics. Participants' re-

sponses controlled the contrast of the stimuli in an adaptive fashion. Logistic functions were fitted to the data to obtain the DKL radius (r) that led to 75% accuracy of discrimination for each condition. Thresholds in terms of r were then transformed into a triplet of Michelson cone-contrast values from which mechanism contrasts were computed to represent the two chromatic mechanisms and the luminance mechanism; see the Data processing section for details.

The study was conducted over several sessions per participant. The first session contained the color vision test and HCFP; this lasted ~30 min. In the main experiment, two 1-hr sessions were conducted to collect the mid-level and high-level thresholds. In the control experiment, a 1-hr session was conducted as only high-level thresholds were collected. In the follow-up experiment, two sessions were again conducted in order to obtain a finer sampling of the luminance elevation angles for contrast combinations involving the L − M mechanism. Breaks were offered to the participants during these sessions and taken when required. In the main experiment, the order of the blocks (mid-level and high-level) was counterbalanced across the sample. Participants who did not reach a threshold of 75% accuracy in the first instance were retested; on average, three out of a total of 20 conditions (10 high-level and 10 mid-level) needed to be retested per participant. This typically included the S − (L + M) high-level isoluminant condition that participants reported to be the most difficult. Two more participants had to be removed at this stage as, even after retesting, it was not possible to measure their high-level thresholds in the isoluminant S − (L + M) direction. These retests were carried out at a later date (approximately 3 to 4 months after the initial testing sessions). The three conditions with a DKL achromatic elevation of 60° were also run at a later date (approximately 2 months after the initial testing was complete) and, similarly to retested conditions, relied on the same stimuli that were previously viewed as we had a limited set of 377 object/nonobject stimuli at our disposal. Therefore, a second set of participants ($n = 12$) was recruited for the control experiment that assessed if the order of testing contributed to the findings as priming effects for object images can potentially be very long-lasting (Mitchell, 2006). These participants were tested with the high-level conditions only. L − M, S − (L + M), and both L − M and S − (L + M) in combination with L + M at a luminance elevation of $\theta_{DKL} = 60°$ were tested before the $\theta_{DKL} = 30°$ combinations.

Because the results of the above experiments revealed some interesting interactions between chromatic and luminance signals (see Results), a follow-up experiment with 15 participants was conducted in order to further study the range of contrasts over which these interactions occur. Thresholds were measured for the high-level task for conditions that combined L − M and L + M and also L − M, S − (L + M), and L + M as well as for the L − M and L + M isolating and L − M with S − (L + M) isoluminant combination. The data were collected in two separate sessions—one for L − M and L + M combined, the other for L − M, S − (L + M), and L + M combined—as the resolution of the luminance elevation was increased to provide thresholds at the following angles $\theta_{DKL} = 0°$, 15°, 30°, 45, 60°, 75°, and 90°. The order of sessions and conditions was counterbalanced across the participants. Two of the participants only completed one of the two sessions, so their data was discarded from the analysis. Further, three participants were removed due to missing data in some of the conditions.

Data processing and statistical analysis

The final sample in the main experiment consisted of 15 participants as we had to exclude three participants due to L − M direction luminance correction angle of 15° or greater (see HCFP section and Supplementary Figure 1) and two participants due to their inability to achieve 75% accuracy within the available gamut for the high-level isoluminant S − (L + M) direction (see Procedure section). The sample in the control experiment consisted of 12 participants, and for the follow-up experiment, 10 participants were included in the final sample (for more detail, see Procedure section).

The measured thresholds expressed in terms of DKL radius (r), chromatic angle (ϕ_{DKL}), and luminance elevation (θ_{DKL}) were converted into L − M, S − (L + M), and L + M mechanism contrasts. This was achieved by measuring the CIE 1931 xyY coordinates of each condition's threshold with a spectroradiometer (SpectroCAL, CRS); these xyY values were converted into CIE XYZ tristimulus values and subsequently into L-, M-, and S-cone excitations. The isoluminant conditions were measured at nominal isoluminance (i.e., elevation of 0°). The conversion of CIE XYZ values into L-, M-, and S-cone excitations was achieved using a 3 × 3 transformation matrix, which was derived according to the method outlined in Golz and MacLeod (2003); the Stockman and Sharpe cone fundamentals (Stockman & Sharpe, 2000; Stockman et al., 1999) along with the measured red, green, and blue spectral power distributions from the Viewsonic P227f CRT monitor guns were used as inputs.

The Michelson cone contrasts ($C_{Michelson}$) were calculated according to Equation 2, where I_{max} and I_{min} are the maxima and minima cone excitations of the Gabors at threshold.

$$C_{Michelson} = \frac{I_{max} - I_{min}}{I_{max} + I_{min}} \quad (2)$$

Mechanism contrasts were then computed for L − M, S − (L + M), and L + M.

As predicted, there were no differences between threshold measurements performed with opposite contrast polarity Gabors, so the data from both staircases for each condition were averaged.

For the main experiment, three repeated measures ANOVAs with the factors of *contrast combination* and *level of task hierarchy* (mid-level or high-level) were conducted on the data: one for S − (L + M), one for L − M, and one for L + M contrast. Combinations with luminance inputs of $\theta_{DKL} = 30°$ and 60° were included in the ANOVAs, resulting in six levels for the *contrast combination* factor for chromatic contrasts (isolating contrast, combination with luminance elevation $\theta_{DKL} =$ 30° and 60°, combination with the other chromatic contrast, combination of all three contrast types with luminance elevation $\theta_{DKL} = 30°$ and 60°) and seven levels for *contrast combination* factor for luminance contrast (isolating contrast, combination with S − (L + M) with luminance elevations of 30° and 60°, combination with L − M with luminance elevation $\theta_{DKL} = 30°$ and 60°, combination of all three contrast types with luminance elevation $\theta_{DKL} = 30°$ and 60°). The Greenhouse-Geisser correction of the degrees of freedom was used when the assumption of sphericity was violated. Tukey's honestly significant difference (HSD) and Bonferroni-corrected paired *t* tests were conducted to further examine the sources of hypothesized differences with the following comparisons being of main interest: (a) Within each mechanism, mid-level and high-level conditions were compared to further examine if their contrast-dependency differed consistently, and (b) the isolating condition was compared to all other conditions at both the mid-level and high level in order to assess if a single channel was driving performance or if there was a facilitation/suppression due to combined signals. A procedure equivalent to a conservative Tukey's HSD test was used in order to take account of the unequally distributed difference variances. The required *t* value was computed as $= Q/\sqrt{2}$ with the *Q* value derived from the studentized range distribution using the Greenhouse-Geisser–corrected degrees of freedom for the tested effect. The Bonferroni correction was applied in addition to Tukey's HSD to obtain the corrected significance values for the corresponding paired *t* tests as Tukey's HSD does not provide these values. We compared the performance of our conservative version of Tukey's HSD with a Bonferroni-corrected *p* value of .05 for 65 comparisons conducted in the main experiment, and it produced almost identical results (only one discrepancy was observed; see Results for details).

A similar approach was used for the control experiment: The differences in threshold contrasts between different contrast combinations—isolating, 30° combination with L − M, 60° combination with L − M, 30° combination with both S − (L + M) and L − M, 60° combination with both S − (L + M) and L − M—were assessed with repeated measures ANOVAs on L − M and L + M contrasts. In the follow-up experiment, L − M and L + M contrast data were subjected to a 6 × 2 repeated measures ANOVA with the factors contrast combination (isolating, 15°, 30°, 45°, 60°, and 75°) and combination type (S − [L + M] excluded or included). Again, Greenhouse-Geisser correction was used when necessary, and Tukey's HSD was used for post hoc tests, correcting the degrees of freedom if the assumption of sphericity was violated.

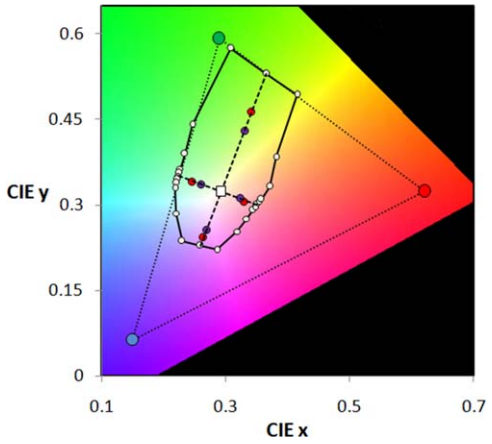

Figure 3. The available gamut of the DKL isoluminant plane is plotted on the CIE 1931 chromaticity diagram. It is bounded by the connected white circles, which indicate points derived from spectroradiometric measurements sampled at every ~15° of azimuth. For comparison, the locations of the RGB display phosphors are indicated. The thresholds for the high-level and mid-level tasks are plotted as red and purple circles, respectively. The white point, i.e., the background, is indicated by the white square. The absolute values of thresholds in the ±(L − M) and ±(S − [L + M]) directions were collapsed and averaged before they were plotted as they did not differ significantly (see Data analysis section).

Results

Main experiment: Mid-level and high-level thresholds for isolating and combined mechanisms

The measured thresholds collapsed across center polarities, i.e., the chromaticity in the center of the Gabor patches, in the ±(S − [L + M]) and ±(L − M) chromatic isolating conditions are shown in Figure 3. The DKL isoluminant plane has been superimposed onto the CIE 1931 space.

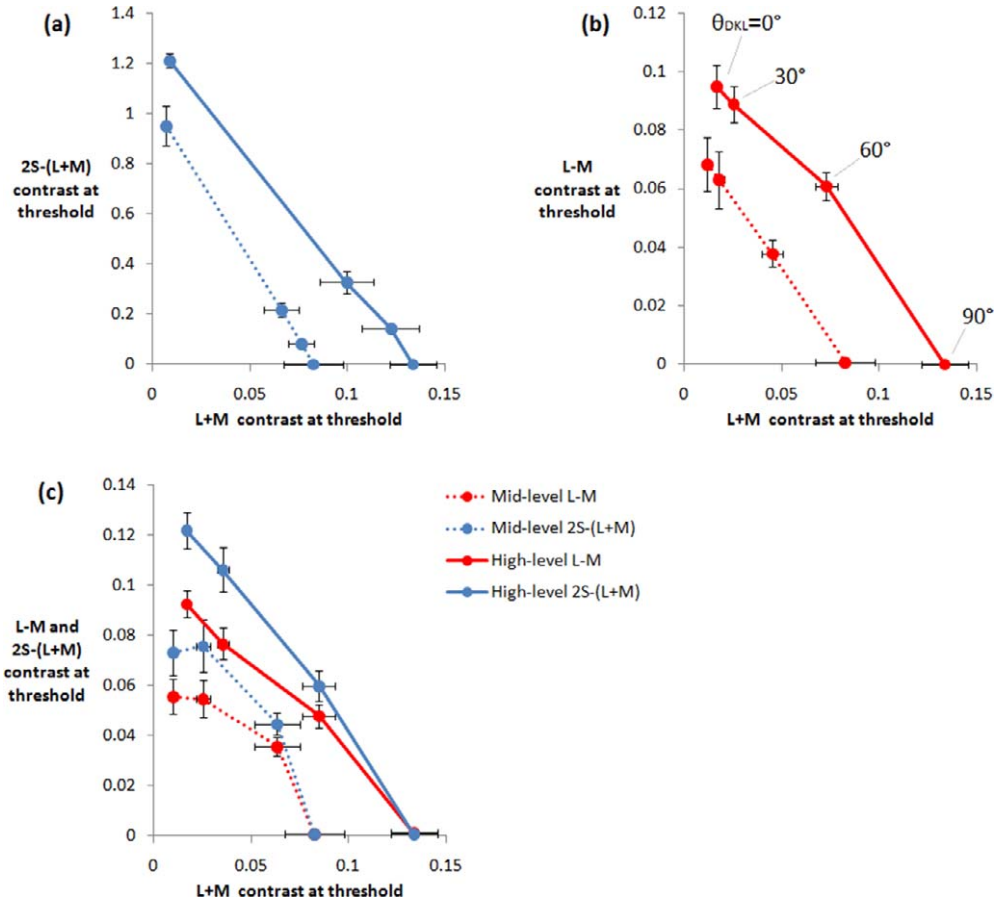

Figure 4. Thresholds from the main experiment as a function of luminance contrast. L − M and 2S − (L + M) thresholds are plotted as red and blue circles, respectively. The mid-level and high-level tasks are indicated by the adjoining dotted and solid lines, respectively. (a) 2S − (L + M) versus L + M thresholds. (b) L − M versus L + M thresholds. (c) Thresholds in both chromatic pathways as a function of L + M thresholds. Note: $\theta_{DKL} = 90°$ corresponds to the luminance isolating condition; this data will fall on the x-axis. $\theta_{DKL} = 0°$ corresponds to the isoluminant condition; this data is the closest to the y-axis in each panel. The corresponding DKL luminance elevations for each data point are indicated in (b) only to avoid clutter. Their order is the same on each plot. Error bars: ±2*SE*.

The mechanism contrasts of the Gabor patches required for threshold (75% accuracy) in the mid-level and high-level discrimination tasks are plotted as function of L + M contrast required for threshold for the S − (L + M), L − M, and combination of L − M and S − (L + M) conditions in Figure 4. Note that, due to the fact that contrasts were derived from spectroradiometric measurements of our stimuli and not simply taken as the assumed contrasts given the definition of the DKL space, tiny deviations from zero do appear in mechanisms that are not meant to be stimulated.

Separate repeated measures ANOVAs were conducted on contrast within every mechanism (S − [L + M], L − M, and L + M) with factors of contrast combination and level of task hierarchy (mid-level and high-level). Significant differences were revealed between the amount of contrast needed to reach threshold in the discrimination tasks at the two levels of visual hierarchy, S − (L + M): $F(1, 14) = 80.25$, $p = 0.000004$, $\eta_p^2 = .85$; L − M: $F(1, 14) = 104.97$, $p = 0.00007$, $\eta_p^2 = .88$; L + M: $F(1, 14) = 119.46$, $p = 0.0000003$, $\eta_p^2 = .90$. This result reflected the increased difficulty and hence the requirement for higher contrast in order to reach threshold when discriminating objects from nonobjects compared to discriminating contours with and without good continuation. In all three cases, there was also a significant difference between contrasts required for different combinations of visual mechanisms: S − (L + M): $F(1.86, 26.16) = 960.40$, $p = 0.006 \times 10^{-22}$, $\eta_p^2 = .99$; L − M: $F(5, 70) = 58.82$, $p = 0.01 \times 10^{-21}$, $\eta_p^2 = .81$; L + M: $F(3.60, 50.38) = 131.37$, $p = 0.03 \times 10^{-23}$, $\eta_p^2 = .90$. This simply means that none of the three channels drove performance in all of the tested conditions. Far more interestingly, interactions between the two factors were present as well: S − (L + M): $F(2.26, 31.66) = 19.36$, $p = 0.00002$, $\eta_p^2 = .58$; L − M: $F(3.06, 42.84) = 5.64$, $p = 0.002$, $\eta_p^2 = .29$; L + M: $F(3.08, 43.16) = 7.85$, $p = 0.0002$, $\eta_p^2 = .36$).

Tukey's HSD and Bonferroni-corrected paired *t* tests were conducted in order to reveal the origin of these

Mechanism	DKL luminance angle (°)	Hierarchy: Mid-level S − (L + M)	Mid-level L − M	Mid-level L + M	High-level S − (L + M)	High-level L − M	High-level L + M
Chromatic isolating	0	**Lower** $t(14) = 22.92$ $p < 0.001$	**Lower** $t(14) = 4.53$ $p < 0.01$	–	Lower $t(14) = 35.92$ $p < 0.001$	Same $t(14) = 0.54$ $p =$ n.s.	–
S − (L + M) & L + M	30	Lower $t(14) = 18.41$ $p < 0.001$	–	Same $t(14) = 1.66$ $p =$ n.s.	Lower $t(14) = 18.51$ $p < 0.001$	–	Same $t(14) = 2.97$ $p =$ n.s.
L − M & L + M	30	–	Same $t(14) = 1.45$ $p =$ n.s.	Lower $t(14) = 9.86$ $p < 0.001$	–	Same $t(14) = 1.17$ $p =$ n.s.	Lower $t(14) = 15.81$ $p < 0.001$
S − (L + M) & L + M	60	Lower $t(14) = 19.00$ $p < 0.001$	–	Same $t(14) = 0.43$ $p =$ n.s.	Lower $t(14) = 30.40$ $p < 0.001$	–	Same $t(14) = -0.94$ $p =$ n.s.
L − M & L + M	60	–	**Lower** $t(14) = 5.20$ $p < 0.005$	**Lower** $t(14) = 4.54$ $p = 0.01$	–	**Lower** $t(14) = 9.74$ $p < 0.001$	**Lower** $t(14) = 6.65$ $p < 0.001$
S − (L + M) & L − M & L + M	30	Lower $t(14) = 22.61$ $p < 0.001$	Same $t(14) = 2.62$ $p =$ n.s.	Lower $t(14) = 8.21$ $p < 0.001$	**Lower** $t(14) = 39.51$ $p < 0.001$	**Lower** $t(14) = 4.80$ $p < 0.01$	**Lower** $t(14) = 13.44$ $p < 0.001$
S − (L + M) & L − M & L + M	60	Lower $t(14) = 23.67$ $p < 0.001$	Lower $t(14) = 5.70$ $p < 0.005$	Same $t(14) = 2.29$ $p =$ n.s.	**Lower** $t(14) = 40.94$ $p < 0.001$	**Lower** $t(14) = 10.26$ $p < 0.001$	**Lower** $t(14) = 4.57$ $p = 0.01$

Table 2. Summary of post hoc *t* tests assessing the relationship between contrasts required for discrimination in isolating condition and combined conditions. *Notes*: In order to allow for easy comparisons with widely used significance levels (0.05, 0.01, 0.005, etc.), we multiplied the actual *p* value with the number of comparisons. "Same" signifies that no significant differences were found between contrasts, indicating that the signal within that mechanism drives performance. "Lower" indicates that contrast within that mechanism was significantly reduced in the combined condition when compared to the isolating condition. The cases in which contrasts in all the channels were lowered by combining the signals are marked by bold text; these are the conditions in which facilitation has occurred. The table indicates that the L + M signal always drives the discrimination when combined with an S – (L + M) signal, but L – M signals drive performance with combined with a relatively low luminance signal (defined at 30°) for the mid-level and also high-level tasks.

differences as described in the Data processing and statistical analysis section. First, differences between mid-level and high-level thresholds were significant in all cases, indicating that their contrast-dependency was consistently different for each mechanism or mechanism combination.[1] Second, the isolating conditions, S − (L + M), L − M, or L + M, were compared to all relevant combined conditions for both mid-level and high-level tasks, revealing the specific determinants for interactions between luminance and chromatic signals. The results of this analysis are summarized in Table 2, which presents differences between performance in combined conditions and performance in the respective isolating condition.

Taken together, these results revealed that luminance signals always drove performance when combined with S − (L + M) signals, independent of mid-level or high-level task. On the other hand, L − M signals drove performance when combined with a luminance signal defined by a luminance elevation of $\theta_{DKL} = 30°$ for both mid-level and high-level tasks. Some facilitatory interactions were also observed. Combinations with all three mechanisms for the high-level task could not be reduced to a single driving channel at both luminance elevations of $\theta_{DKL} = 30°$ and 60°. This was also the case for L − M and luminance at an elevation of $\theta_{DKL} = 60°$, i.e., an interaction existed, between the L − M and L + M signals when the luminance elevation was $\theta_{DKL} = 60°$, which did not exist when it was $\theta_{DKL} = 30°$. The chromatic combination of L − M and S − (L + M) was also facilitatory but for the mid-level task only.

Control experiment: High-level task with 60° elevation thresholds measured before 30° thresholds

As mentioned in the Methods section, combinations at $\theta_{DKL} = 60°$ were measured after $\theta_{DKL} = 30°$ and involved a subset of the same stimuli. To check if the

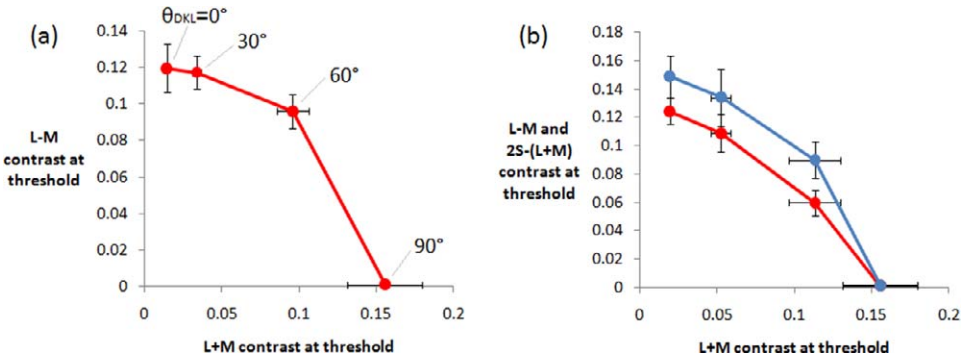

Figure 5. Thresholds as a function of luminance contrast from the control experiment, which contained the high-level task only. (a) L − M versus L + M thresholds. (b) Combined 2S −(L + M) and L − M contrasts at threshold as a function of L + M contrast at threshold. Note: $\theta_{DKL} = 90°$ corresponds to the luminance isolating condition; this data will fall on the x-axis. $\theta_{DKL} = 0°$ corresponds to the isoluminant condition; this data is the closest to the y-axis in each panel. The corresponding DKL luminance elevations for each data point are indicated in (a) only to avoid clutter. Error bars: ±2*SE*.

results were influenced by the potential order confound, we conducted a control experiment with high-level conditions on a separate sample of 12 participants. The results are plotted in Figure 5. We performed repeated measures ANOVAs on L − M and L + M contrasts with the sole factor being contrast combination (isolating, 30° elevation combination with L − M, 60° elevation combination with L − M, 30° elevation combination with both S − [L + M] and L − M, 60° elevation combination with both S − [L + M] and L − M). Both ANOVAs showed significant differences, L–M: $F(1.67, 16.74) = 29.82$, $p = 0.00006$, $\eta_p^2 = .75$; L + M: $F(1.59, 15.89) = 45.52$, $p = 0.000001$, $\eta_p^2 = .82$. Tukey's HSD test was used for closer testing of the interactions between channels. No significant differences were found between the L − M isolating condition and the L − M combined with luminance at 30° elevation, indicating that the L − M signal was driving performance. Facilitations between luminance and L − M signals were again found for L − M combined with L + M signals at $\theta_{DKL} = 60°$. An interaction was not found for a combination of all three mechanisms at $\theta_{DKL} = 30°$, with the L − M mechanism found to be driving performance, or at $\theta_{DKL} = 60°$, with luminance found to be driving performance. The control experiment thus partly replicated the findings of the main experiment, finding an interaction between a combination of L − M and luminance signals at 60° elevation that could not be reduced to order effects.

Follow-up experiment: High-level task with a narrower sampling of DKL elevation

In order to pinpoint the range of DKL elevation angles at which an interaction between channels can occur, we conducted a follow-up experiment with high-level stimuli. In this experiment, the DKL angle resolution for L − M and L + M as well as for S − (L + M), L − M, and L + M was doubled to 15° as can be seen from Figure 6. Repeated measures ANOVAs with the factor contrast combination (isolating, 15°, 30°, 45°, 60°, and 75° combination) and presence of S − (L + M) contrast in the combination (absent or present) were conducted on L − M and L + M contrasts required for threshold. Large, significant differences in contrasts required to reach threshold between different contrast combinations were found, L − M: $F(5, 45) = 109.14$, $p < 0.0000001$, $\eta_p^2 = .92$; L + M: $F(1.85, 16.66) = 103.45$, $p < 0.0000001$, $\eta_p^2 = .92$. There were also strong tendencies for differences between the combinations that did and did not involve the S − (L + M) mechanism, L − M: $F(1, 9) = 4.84$, $p = 0.055$, $\eta_p^2 = .35$; L + M: $F(1, 9) = 5.59$, $p = 0.042$, $\eta_p^2 = .38$. The main effects were further qualified by a significant interaction, L − M: $F(5, 45) = 2.63$, $p = 0.036$, $\eta_p^2 = .23$; L + M: $F(2.73, 24.53) = 5.58$, $p = 0.006$, $\eta_p^2 = .38$. Tukey's HSD test revealed that a facilitation between contrasts occurred at 45° when L − M was combined with luminance as both thresholds were lower than in the respective isolating conditions. For the combination of all three mechanisms, facilitation occurred at both 45° and 60° of elevation. The contrasts needed for threshold in the two experiments were very similar. The only significant difference between them occurred for L − M contrast at 75° elevation, which was significantly higher in the L − M with L + M condition. However, this is very likely an artifact of the way that signals are increased along different directions of the DKL space (see Methods) and does not have functional significance as luminance contrast was found to be driving performance in this condition.

Plots that allow for comparisons between mean mid-level and high-level thresholds for the S − (L + M), L − M, and L + M mechanisms are shown in Figure 7. Considering the mechanisms contributing to the discrimination process in the mid-level versus high-level

tasks (either driving the performance or participating in an interaction; see Table 2) revealed the following: the L − M contrasts at threshold remained very similar irrespective of the condition from which they are derived (Figure 7b), forming a cluster in which high-level L − M thresholds were on average ~1.2 times the magnitude of the mid-level L − M thresholds. On the contrary, Figure 7c, depicting the L + M contrasts, revealed that the L + M mechanism could reach threshold over a range of contrasts and that a linear relationship ($R^2 = 0.93$, $p < 0.05$) existed between these mid-level thresholds and the corresponding high-level thresholds. The high-level L + M thresholds were 1.4 times the mid-level L + M thresholds. There was only one condition in which the S − (L + M) mechanism drove discrimination: This was the S − (L + M) isolating condition in which no other channels were activated (Figure 7a).

Discussion

This study psychophysically assessed the contributions of the chromatic cone-opponent channels and the luminance channel to mid-level and high-level visual processing. We used comparable stimulus setups for the two tasks, relying on Gaborized stimuli that required either contour continuation discrimination or discrimination between nameable objects and unnameable, novel objects ("nonobjects"). Predictably, high-level object discrimination required more contrast than the mid-level discrimination task. However, the main findings concern interactions between different channels, which are especially prominent at the high-level stage of vision. L − M signals can play an important role in high-level vision, driving the performance when joined with relatively weak luminance signals and also entering into facilitatory interactions with luminance signals that fall into a limited, relatively low L + M contrast range (approximately 0.05–0.09). Furthermore, clear relationships were found between mean mid-level and high-level performance across the sample with luminance contrasts that contributed to performance at threshold being linearly distributed and L − M contrasts being somewhat less variable. This complements the findings of previous studies demonstrating that the luminance-sensitive detection mechanism receives L − M input but not vice versa (Cass, Clifford, Alais, & Spehar, 2009), indicating an asymmetric interaction between the L − M and L + M mechanisms (see also Cole et al., 1990). However, we now demonstrate for the first time that this asymmetry may extend to the highest level of the visual hierarchy.

Another finding was that S-cones were very ineffective when high-level discrimination was needed and did

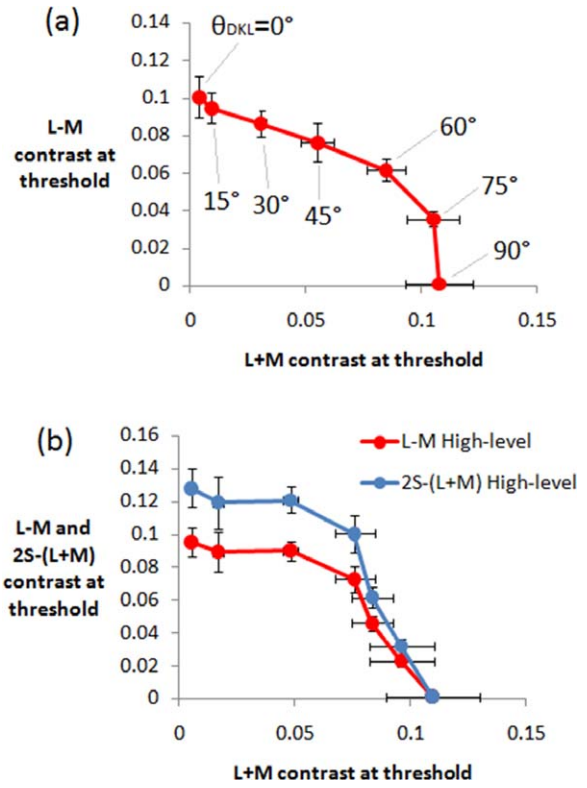

Figure 6. Thresholds as a function of luminance contrast from the follow-up experiment, which contained the high-level task only and used a more narrow sampling of the DKL angle of elevation. (a) L − M versus L + M thresholds. (b) Combined 2S – (L + M) and L − M contrasts at threshold as a function of L + M contrast at threshold. (a) indicates the DKL luminance elevations that correspond to each data point; their order is the same as on (b), on which they are left out to avoid clutter. Error bars: ±2*SE*.

not contribute to performance in any of the conditions combining them with more salient L + M signals. However, an interaction between the two chromatic signals alone was observed in mid-level vision, indicating that S − (L + M) signals might facilitate L − M signals that remain relatively weak (approximately 0.06 L − M contrast). For L − M signals, performance was found to be as effective for an isolating stimulus as it was for a combination of luminance and L − M when luminance signals were weak (0.02–0.03 of L + M contrast). On the other hand, in the combined conditions that favored somewhat larger luminance signals, interactions between luminance and L − M signals were observed. Less luminance contrast was required for these combined conditions as opposed to the luminance-isolating condition. Here, luminance levels spanned 0.05–0.09 of L + M contrast. Pelli (2011) asked why humans require so much contrast to recognize complex objects and why they perform much less optimally than the ideal observer. Our findings imply that, in situations of reduced contrast, it may be

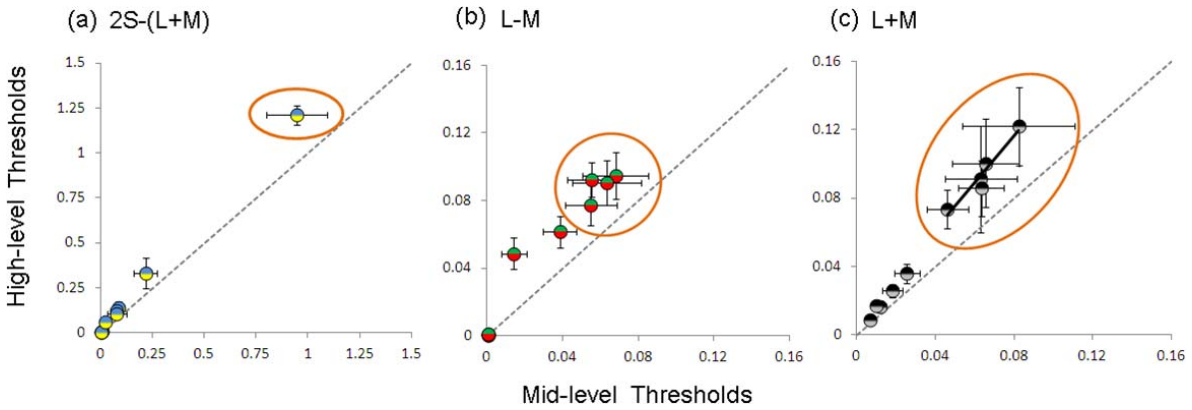

Figure 7. Relationships between mean mid-level and high-level thresholds. The graphs illustrated by (a, b, and c) show the measured thresholds for the high-level task (ordinate) as a function of threshold for the mid-level tasks for the S − (L + M), L − M, and L + M mechanisms, respectively (abscissa). The orange ellipses were drawn onto the graphs in order to highlight the thresholds for which the given mechanism is contributing to the discrimination. The points outside of the orange ellipses belong to combined contrast conditions in which performance was driven by another mechanism. The linear relationship shown in (c) is defined by High = 1.4* Mid ($R^2 = 0.93$, $p < 0.05$). Note: Thresholds expressed in terms of mechanism contrasts computed from Michelson cone contrasts.

useful to pool information from several channels in order to optimize performance. A model that proposes a use for color contrast that is separate from simply defining appearance was proposed by Shapiro (2008). Experimental support for pooling of contrast across mechanisms in natural scene classification was recently provided (Groen, Ghebreab, Lamme, & Scholte, 2012). The pooling of these signals could happen at a decision stage, based on information from independent channels, or within a specialized system that is responsive to both types of contrast.

Physiologically, L − M signals could play a role in mid-level and high-level vision through L − M edge detectors (Shapley & Hawken, 2011), multiplexed chromatic and luminance signals (Kingdom & Mullen, 1995), or both. Although the parvocellular-based, cone-opponent L − M mechanism provides signals that can be multiplexed with luminance information as reported, among others, by Derrington et al. (1984), recent studies indicate that this processing strategy is not utilized when coding stimuli that combine luminance and chromatic inputs in complex structural patterns (Cooper, Sun, & Lee, 2012; Lee, Sun, & Valberg, 2011). Strict subcortical segregation of luminance and L − M signals has already been proposed as a useful strategy for optimizing signal transmission in a noisy bandwith-limited system (e.g., von der Twer & MacLeod, 2001). This leaves the L − M edge detectors as the likely candidate for the physiological substrate of the observed effects. Mullen and Beaudot (2002) found that global shape discrimination is not pronouncedly worse for stimuli defined with chromatic-only signals, discussing as the likely physiological substrate both L − M edge detectors in V1 and V2 and area V4, which is sensitive to both color and shape information.

Another, perhaps simpler explanation would be that color signals were aiding performance when luminance signals were relatively weak by contributing to conspicuousness. Still, it is not clear why an improvement of conspicuousness would only occur for a combination of L − M signals with luminance and not for the S − (L + M) signals when, in the natural world, S-cone signals are also widely used for conspicuousness (e.g., Renoult, Schaefer, Salle, & Charpentier, 2011). It is highly likely that the object discrimination task was particularly challenging for the S − (L + M) system, which is less suited for form perception due to its lower spatial resolution (Calkins, 2001). This is supported by the fact that two participants in the main experiment had to be discarded due to their inability to reach threshold within the available gamut for the S − (L + M) isolating condition, and several others needed to be retested in this condition at a later date in order to obtain valid data. Furthermore, Figure 4a shows that the S − (L + M) isolating contrast at threshold is several orders of magnitude above the S − (L + M) contrast present at the 30° elevation threshold. It may be possible that at a lower range of DKL elevations, allowing for higher S − (L + M) contrasts, interactions will be observed between S − (L + M) and L + M signals. Also, as reviewed by Gegenfurtner (2003), geniculate neurons sensitive to S − (L + M) signals are optimally sensitive to luminance at angles of elevation between approximately 0° and 20°. The possibility of interactions between luminance and S − (L + M) signals needs to be examined in a further study, possibly focused around $\theta_{DKL} = 15°$ for the S − (L + M) and L + M combinations.

A similar alternative explanation relates to cross-channel luminance and chromatic contrast masking. As

summarized in the Introduction, research on effects of simultaneous overlay cross-channel masking on contrast detection thresholds has found evidence of asymmetric masking when thresholds in one channel were measured in the presence of suprathreshold contrast in the other channel with luminance facilitating chromatic L − M signals and color masking luminance signals (e.g., Cole, Hine, & McIlhagga, 1993). However, one should also consider that Stromeyer, Thabet, Chaparro, and Kronauer (1999) and Cole et al. (1990) both argued that facilitatory cross-channel effects are very likely to be the result of spatial cues enhancing the detectability of cross-channel contrast. For example, in Cole et al. (1990), the masking is only observed when the mask extended spatially beyond the test patch, thus allowing the luminance contrast to facilitate detection of chromatic variation by spatially demarcating it. In our study, contrasts from different channels were combined in a single Gabor patch with no spatial discontinuities, but we still found a series of facilitatory interactions. Furthermore, for most DKL elevations in our study (see Figures 4 through 6), both luminance and chromatic threshold contrasts were highly likely to be many times above detection threshold. To our knowledge, there are few studies that examined suprathreshold contrast interactions. In one of them, Kingdom, Bell, Gheorghiu, and Malkoc (2010) demonstrated that suprathreshold color variations suppress suprathreshold brightness variations. Further research should establish the relationship between discrimination and detection thresholds from combined channel contrasts as well as extend our knowledge of suprathreshold color/luminance contrast masking as low-level interactions between contrasts could perhaps partly account for the data obtained in studies that aim to examine putative mid-level or high-level visual phenomena (e.g., Clery, Bloj, & Harris, 2013).

The characteristics of the spatially variable object and nonobject images should also be considered. Traditional psychophysics experiments rely on stimulus sets whose properties are highly controlled. An analysis of the high-level stimulus set revealed that the object stimuli contained significantly more vertical and horizontal components relative to the nonobject stimuli. Due to the oblique effect, participants could have been more sensitive to structure within the object stimuli aligned to their vertical or horizontal axes of symmetry. However, a previous ERP study (Martinovic et al., 2011) that employed object and nonobject line drawing stimuli showed that the magnitude of the N1 component was greater for nonobjects relative to objects. This goes contrary to the expected N1 enhancement for horizontal/vertical orientations (e.g., Song et al., 2010). In addition, the mid-level task contour stimuli contained no orientation bias, but there was still a clear linear relationship between the mid-level and high-level L + M contrasts at threshold (see Figure 7). This is not consistent with a dominant contribution from a low-level orientation artefact but speaks more in favor of a connection between tasks, at least at the level of perceptual organization.

The mid-level task could have also been affected by a potential confound. In order to judge whether a contour possessed good continuation, participants could have been comparing only the four Gabor patches that immediately surrounded the central Gabor patch located approximately at the fixation point and hence not processing the entire contour as intended. The consequence of this is that the task can be reduced to orientation matching at the intersection in order to assess for presence or absence of good continuation. If this strategy were used during the task, it would still have, however, corresponded to the correct hierarchal level of processing (mid-level). This is supported by the results as the systematic upward shift in thresholds for all channels from the mid-level to high-level tasks indicates that there is a clear relationship between them.

Based on our findings, it is highly likely that integrative processes in high-level vision depend on information from all visual channels and not just on luminance. Upstream visual cortical areas that subserve object processing, e.g., the lateral occipital cortex (Grill-Spector & Malach, 2004) receive a broad range of cortical inputs, containing magnocellular and parvocellular inputs in about equal measure (Leonards & Singer, 1998). However, the exact nature of early cortical interactions that involve luminance and, therefore, are crucial for object vision has not been studied yet. This study establishes fundamental psychophysical evidence that demonstrates specific contrast level–dependent luminance and chromatic interactions in high-level visual processing and provides a suitable stimulus set and contrast threshold data that could facilitate future neuroimaging studies.

Keywords: object classification, good continuation, perceptual organization, luminance, color, postreceptoral mechanisms, visual pathways

Acknowledgments

The work was supported by BBSRC new investigator grant BB/H019731/1 to JM.

Commercial relationships: none.
Corresponding author: Jasna Martinovic.
Email: j.martinovic@abdn.ac.uk.
Address: School of Psychology, University of Aberdeen, Aberdeen, UK.

Footnote

[1]The only discrepancy between the conservative version of Tukey's HSD and Bonferroni correction appeared here—although all mid-level and high-level thresholds were different according to Tukey's HSD, Bonferroni correction indicated that the mid-level and high-level thresholds were the same for a combination of S − (L + M) and L + M contrast at 30° elevation.

References

Alario, F. X., & Ferrand, L. (1999). A set of 400 pictures standardized for French: Norms for name agreement, image agreement, familiarity, visual complexity, image variability, and age of acquisition. *Behavior Research Methods, Instruments, and Computers, 31,* 531–552.

Bar, M. (2003). A cortical mechanism for triggering top-down facilitation in visual object recognition. *Journal of Cognitive Neuroscience, 15,* 600–609.

Bar, M., Kassam, K. S., Ghuman, A. S., Boshyan, J., Schmid, A. M., Dale, A. M., ... Halgren, E. (2006). Top-down facilitation of visual recognition. *Proceedings of the National Academy of Sciences, USA, 103,* 449–454.

Bates, E., D'Amico, S., Jacobsen, T., Szekely, A., Andonova, E., Devescovi, A., ... Tzeng, O. (2003). Timed picture naming in seven languages. *Psychonomic Bulletin & Review, 10,* 344–380.

Beaudot, W. H. A., & Mullen, K. T. (2001). Processing time of contour integration: The role of colour, contrast, and curvature. *Perception, 30*(7), 833–853.

Beaudot, W. H. A., & Mullen, K. T. (2003). How long range is contour integration in human color vision? *Visual Neuroscience*, *20*(1), 51–64.

Brainard, D. H., Roorda, A., Yamauchi, Y., Calderone, J. B., Metha, A., Neitz, M., ... Jacobs, G. H. (2000). Functional consequences of the relative numbers of L and M cones. *Journal of the Optical Society of America A: Optics, Image Science, and Vision, 17*(3), 607–614.

Calkins, D. J. (2001). Seeing with S cones. *Progress in Retinal and Eye Research*, *20*(3), 255–287.

Campbell, F. W., & Robson, J. (1968). Application of Fourier analysis to the visibility of gratings. *Journal of Physiology, 197,* 551–566.

Cant, J. S., Large, M. E., McCall, L., & Goodale, M. A. (2008). Independent processing of form, colour, and texture in object perception. *Perception*, *37*(1), 57–78.

Cass, J., Clifford, C. W. G., Alais, D., & Spehar, B. (2009). Temporal structure of chromatic channels revealed through masking. *Journal of Vision, 9*(5): 17, 1–15, http://www.journalofvision.org/content/9/5/17, doi:10.1167/9.5.17. [PubMed] [Article]

Clery, S., Bloj, M., & Harris, J. M. (2013). Interactions between luminance and color signals: Effects on shape. *Journal of Vision, 13*(5):16, 1–23, http://www.journalofvision.org/content/13/5/16, doi:10.1167/13.5.16. [PubMed] [Article]

Cole, G. R., Hine, T., & McIlhagga, W. (1993). Detection mechanisms in L-cone, M-cone and S-cone contrast space. *Journal of the Optical Society of America A: Optics, Image Science, and Vision, 10*(1), 38–51.

Cole, G. R., Stromeyer, C. F., & Kronauer, R. E. (1990). Visual interactions with luminance and chromatic stimuli. *Journal of the Optical Society of America A: Optics, Image Science, and Vision, 7*(1), 128–140.

Cooper, B., Sun, H., & Lee, B. B. (2012). Psychophysical and physiological responses to gratings with luminance and chromatic components of different spatial frequencies. *Journal of the Optical Society of America A: Optics, Image Science, and Vision, 29*(2), A314–A323.

Crognale, M. A. (2002). Development, maturation, and aging of chromatic visual pathways: VEP results. *Journal of Vision, 2*(6):2, 438–450, http://www.journalofvision.org/content/2/6/2, doi:10.1167/2.6.2. [PubMed] [Article]

Derrington, A. M., Krauskopf, J., & Lennie, P. (1984). Chromatic mechanisms in lateral geniculate nucleus of macaque. *Journal of Physiology, 357,* 241–265.

DiCarlo, J. J., Zoccolan, D., & Rust, N. C. (2012). How does the brain solve visual object recognition? *Neuron, 73*(3), 415–434.

Dobkins, K. R., Thiele, A., & Albright, T. D. (2000). Comparison of red-green equiluminance points in humans and macaques: Evidence for different L : M cone ratios between species. *Journal of the Optical Society of America A: Optics, Image Science, and Vision, 17*(3), 545–556.

Gegenfurtner, K. R. (2003). Cortical mechanisms of colour vision. *Nature Reviews Neuroscience*, *4*(7), 563–572.

Gegenfurtner, K. R., & Hawken, M. J. (1995). Temporal and chromatic properties of motion mechanisms. *Vision Research*, *35*(11), 1547–1563.

Gegenfurtner, K. R., & Kiper, D. C. (2003). Color vision. *Annual Review of Neuroscience, 26,* 181–206.

Goldstone, R. L., Gerganov, A., Landy, D., & Roberts, M. E. (2009). Learning to see and conceive. In L.

Tommasi, M. Peterson, & L. Nadel (Eds.), *The new cognitive sciences* (pp. 163–188). Cambridge, MA: MIT Press.

Golz, J., & MacLeod, D. I. A. (2003). Colorimetry for CRT displays. *Journal of the Optical Society of America A: Optics, Image Science, and Vision*, *20*, 769–781.

Grill-Spector, K., & Malach, R. (2004). The human visual cortex. *Annual Review of Neuroscience, 27,* 649–677.

Groen, I. I. A., Ghebreab, S., Lamme, V. A. F., & Scholte, H. S. (2012). Spatially pooled contrast responses predict neural and perceptual similarity of naturalistic image categories. *PLoS Computational Biology, 8*(10), e1002726.

Hamm, J. P., & McMullen, P. A. (1998). Effects of orientation on the identification of rotated objects depend on the level of identity. *Journal of Experimental Psychology: Human Perception and Performance, 24,* 413–426.

Hansen, T., & Gegenfurtner, K. F. (2009). Independence of color and luminance edges in natural scenes. *Visual Neuroscience*, *26*(1), 35–49.

Kaiser, P. K. (1971). Minimally distinct border as a preferred psychophysical criterion in visual heterochromatic photometry. *Journal of the Optical Society of America A*, *61*(7), 966–971.

Kaiser, P. K., Lee, B. B., Martin, P. R., & Valberg, A. (1990). The physiological basis of the minimally distinct border demonstrated in the ganglion cells of the macaque retina. *Journal of Physiology, 422*, 153–183.

Kingdom, F. A. A., Bell, J., Gheorghiu, E., & Malkoc, G. (2010). Chromatic variations suppress suprathreshold brightness variations. *Journal of Vision, 10*(10):13, 1–13, http://www.journalofvision.org/content/10/10/13, doi:10.1167/10.10.13. [PubMed] [Article]

Kingdom, F. A. A., & Mullen, K. T. (1995). Separating colour and luminance information in the visual system. *Spatial Vision*, *9*(2), 191–219.

Kingdom, F. A. A., & Prins, N. (2009). *Psychophysics: A practical introduction*. London: Academic Press.

Kulikowski, J. J. (2003). Neural basis of fundamental filters in vision. In G. T. Buracas, O. Ruksenas, G. M. Boynton, & T. D. Albright (Eds.), *Modulation of neuronal signalling: Implications for active vision,*Vol. 334 (pp. 3–68). Dordrecht: NATO Science Series, Life Sciences.

Kveraga, K., Boshyan, J., & Bar, M. (2007). Magnocellular projections as the trigger of top-down facilitation in recognition. *Journal of Neuroscience*, *27*(48), 13232–13240.

Lee, B. B., Sun, H., & Valberg, A. (2011). Segregation of chromatic and luminance signals using a novel grating stimulus. *Journal of Physiology-London*, *589*(1), 59–73.

Leonards, U., & Singer, W. (1998). Two texture segregation mechanisms with differential sensitivity for colour and luminance contrast. *Vision Research, 38,* 101–109.

Mandelli, M. J. F., & Kiper, D. C. (2005). The local and global processing of chromatic Glass patterns. *Journal of Vision, 5*(5):2, 405–416, http://www.journalofvision.org/content/5/5/2, doi:10.1167/5.5.2. [PubMed] [Article]

Martinovic, J., Mordal, J., & Wuerger, S. M. (2011). Event-related potentials reveal an early advantage for luminance contours in the processing of objects. *Journal of Vision, 11*(7):1, 1–15, http://www.journalofvision.org/content/11/7/1, doi:10.1167/11.7.1. [PubMed] [Article]

Mathes, B., & Fahle, M. (2007). The electrophysiological correlate of contour integration is similar for color and luminance mechanisms. *Psychophysiology*, *44*(2), 305–322.

McKeefry, D. J., Murray, I. J., & Kulikowski, J. J. (2001). Red-green and blue-yellow mechanisms are matched in sensitivity for temporal and spatial modulation. *Vision Research, 41,* 245–255.

Mitchell, D. B. (2006). Nonconscious priming after 17 years - Invulnerable implicit memory? *Psychological Science*, *17*(11), 925–929.

Mullen, K. T., & Beaudot, W. H. A. (2002). Comparison of color and luminance vision on a global shape discrimination task. *Vision Research*, *42*(5), 565–575.

Mullen, K. T., Beaudot, W. H. A., & McIlhagga, W. H. (2000). Contour integration in color vision: A common process for the blue-yellow, red-green and luminance mechanisms? *Vision Research, 40*(6), 639–655.

Palmer, S. E. (1999). *Vision science: Photons to phenomenology*. Cambridge, MA: MIT Press.

Palmer, S. E., & Brooks, J. L. (2008). Edge-region grouping in figure-ground organization and depth perception. *Journal of Experimental Psychology-Human Perception and Performance, 34*(6), 1353–1371.

Pearson, P. M., & Kingdom, F. A. A. (2002). Texture-orientation mechanisms pool colour and luminance contrast. *Vision Research*, *42*(12), 1547–1558.

Pelli, D. (2011). Visual sensitivity explained [Abstract]. *Perception ECVP Abstract Supplement, 40*, 15.

Peterson, M. A., & Gibson, B. S. (1993). Shape recognition contributions to figure-ground organi-

sation in three-dimensional displays. *Cognitive Psychology, 25,* 383–429.

Peterson, M. A., & Gibson, B. S. (1994). Object recognition contributions to figure-ground organization: Operations on outlines and subjective contours. *Perception & Psychophysics, 56,* 551–564.

Regan, B. C., Reffin, J. P., & Mollon, J. D. (1994). Luminance noise and the rapid determination of discrimination ellipses in color deficiency. *Vision Research*, *34*(10), 1279–1299.

Renoult, J. P., Schaefer, H. M., Salle, B., & Charpentier, M. J. E. (2011). The evolution of the multicoloured face of mandrills: Insights from the perceptual space of colour vision. *PLoS ONE, 6*(12), e29117.

Sassi, M., Vancleef, K., Machilsen, B., Panis, S., & Wagemans, J. (2010). Identification of everyday objects on the basis of Gaborized outline versions. *i-Perception*, *1*(3), 121–142.

Shapiro, A. G. (2008). Separating color from color contrast. *Journal of Vision, 8*(1):8, 1–18, http://www.journalofvision.org/content/8/1/8, doi:10.1167/8.1.8. [PubMed] [Article]

Shapley, R., & Hawken, M. J. (2011). Color in the cortex: Single- and double-opponent cells. *Vision Research, 51*(7), 701–717.

Shevell, S. K., & Kingdom, F. A. A. (2008). Color in complex scenes. *Annual Review of Psychology, 59,* 143–166.

Solomon, S. G., & Lennie, P. (2007). The machinery of colour vision. *Nature Reviews Neuroscience*, *8*(4), 276–286.

Song, Y., Sun, L., Wang, Y., Zhang, X. M., Kang, J., Ma, X. L., … Ding, Y. L. (2010). The effect of short-term training on cardinal and oblique orientation discrimination: An ERP study. *International Journal of Psychophysiology, 75*(3), 241–248.

Stockman, A., & Sharpe, L. T. (2000). Spectral sensitivities of the middle- and long-wavelength sensitive cones derived from measurements in observers of known genotype. *Vision Research, 40,* 1711–1737.

Stockman, A., Sharpe, L. T., & Fach, C. (1999). The spectral sensitivity of the human short-wavelength sensitive cones derived from thresholds and color matches. *Vision Research*, *39*(17), 2901–2927.

Stromeyer, C. F., Chaparro, A., Tolias, A. S., & Kronauer, R. E. (1997). Colour adaptation modifies the long-wave versus middle-wave cone weights and temporal phases in human luminance (but not red-green) mechanism. *Journal of Physiology-London*, *499*(1), 227–254.

Stromeyer, C. F., Thabet, R., Chaparro, A., & Kronauer, R. E. (1999). Spatial masking does not reveal mechanisms selective to combined luminance and red-green color. *Vision Research*, *39*(12), 2099–2112.

Switkes, E., Bradley, A., & DeValois, K. K. (1988). Contrast dependence and mechanisms of masking interactions among chromatic and luminance gratings. *Journal of the Optical Society of America A, 5,* 385–402.

Szekely, A., & Bates, E. (2000). Objective visual complexity as a variable in studies of picture naming [Electronic Version]. *Center for Research in Language Newsletter*, *12*. Retrieved from http://www.crl.ucsd.edu/newsletter/12-2/article.html

Tailby, C., Szmajda, B. A., Buzas, P., Lee, B. B., & Martin, P. R. (2008). Transmission of blue (S) cone signals through the primate lateral geniculate nucleus. *Journal of Physiology-London*, *586*(24), 5947–5967.

Victor, J. D., Purpura, K. P., & Conte, M. M. (1998). Chromatic and luminance interactions in spatial contrast signals. *Visual Neuroscience, 15,* 607–624.

Vidyasagar, T. R., Kulikowski, J. J., Lipnicki, D. M., & Dreher, B. (2002). Convergence of parvocellular and magnocellular information channels in the primary visual cortex of the macaque. *European Journal of Neuroscience*, *16*(5), 945–956.

von der Twer, T., & MacLeod, D. I. A. (2001). Optimal nonlinear codes for the perception of natural colours. *Network-Computation in Neural Systems*, *12*(3), 395–407.

Wagner, G., & Boynton, R. M. (1972). Comparison of four methods of heterochromatic photometry, *Journal of the Optical Society of America A*, *62*(12), 1508–1515.

Walsh, J. W. T. (1958). *Photometry* (3rd ed.). London, UK: Constable & Co. Ltd.

Westland, S., Ripamonti, C., & Cheung, V. (2012). *Computational colour science using MATLAB* (2nd ed.). Chichester, NY: John Wiley & Sons.

Wilson, J. A., & Switkes, E. (2005). Integration of differing chromaticities in early and mid-level spatial vision. *Journal of the Optical Society of America A: Optics, Image Science, and Vision, 22*(10), 2169–2181.

Wuerger, S. M., & Morgan, M. J. (1999). The input of the long- and medium wavelength sensitive cones to orientation discrimination. *Journal of the Optical Society of America*, *16*(3), 436–442.

Wyszecki, G., & Stiles, W. S. (2000). *Color science: Concepts and methods, quantitative data and formulae* (2nd ed.). New York: John Wiley & Sons.